

This article appeared in a journal published by Elsevier. The attached copy is furnished to the author for internal non-commercial research and education use, including for instruction at the authors institution and sharing with colleagues.

Other uses, including reproduction and distribution, or selling or licensing copies, or posting to personal, institutional or third party websites are prohibited.

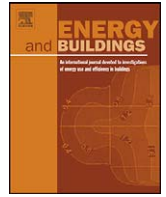
In most cases authors are permitted to post their version of the article (e.g. in Word or Tex form) to their personal website or institutional repository. Authors requiring further information regarding Elsevier's archiving and manuscript policies are encouraged to visit:

<http://www.elsevier.com/copyright>



Contents lists available at ScienceDirect

Energy and Buildings

journal homepage: [www.elsevier.com/locate/enbuild](http://www.elsevier.com/locate/enbuild)

# Parameters optimization of a vertical ground heat exchanger based on response surface methodology

Vahid Khalajzadeh<sup>a</sup>, Ghassem Heidarinejad<sup>a,\*</sup>, Jelena Srebric<sup>b</sup>

<sup>a</sup> Department of Mechanical Engineering, Tarbiat Modares University, P.O. Box 14115-143, Tehran, Iran

<sup>b</sup> Department of Architectural Engineering, Pennsylvania State University, PA 16802, USA

## ARTICLE INFO

### Article history:

Received 11 July 2010

Received in revised form 10 January 2011

Accepted 12 January 2011

### Keywords:

Vertical ground heat exchanger (VGHE)

Computational fluid dynamics (CFD)

Response Surface Model (RSM)

Central Composite Design (CCD)

Optimization

## ABSTRACT

Vertical ground heat exchangers are one of the most important parts of geothermal utilization systems. In order to understand the effect of simultaneous variation of design parameters; a three dimensional computational fluid dynamics simulation was carried out. Based on the effective parameters on the heat exchanger efficiency and the total heat transfer efficiency in cooling mode, and with the aid of the second-order Response Surface Model, two functions for the total heat transfer efficiency and the heat exchanger efficiency were derived. The effects of different design parameters on the response variables were examined. Based on the Response Surface Model, it was found that the dimensionless inlet fluid temperature and the dimensionless pipe diameter significantly affect the response variables, while the response variables are weakly affected by dimensionless depth. Finally, an optimization was performed and the optimum heat exchanger is defined using the model equations.

© 2011 Elsevier B.V. All rights reserved.

## 1. Introduction

With vertical ground heat exchangers (VGHEs), illustrated in Fig. 1, heat is exchanged to the underground environment to provide cooling or heating. VGHEs are being used for an increasing number of applications such as space heating or cooling, water heating, crop drying, agricultural greenhouses, etc. During the heat transfer process, several parameters known as design parameters could affect the VGHE efficiency. Main parameters include deep ground temperature, mass flow rate, and borehole depth. In order to understand the effect of different parameters on the heat transfer efficiency and the heat exchanger efficiency, a large number of experimental measurements are needed. As a result, the total cost of the experiment would be too high. Consequently, some numerical methods, like computational fluid dynamics (CFD) have been helping engineers the past few decades. Several numerical and analytical methods have been reported by Mei and Emerson [1], Muraya et al. [2], Rottmayer et al. [3], Thornton et al. [4], Li et al. [5], Gao et al. [6], Cui et al. [7], Lee and Lam [8] and Li and Zheng [9].

Kavanaugh [10] used a two-dimensional finite-difference method to study the performance of a borehole with a concentric tube. Eskilson and Claesson [11] calculated the ground temperature

around a VGHE using a two-dimensional explicit finite difference method. He proposed G-functions for a long-term step, and later Yavuzturk et al. [12,13] proposed a short-term step-response factor method. The short-time step model of Yavuzturk et al. utilized an automated parametric grid generation algorithm for different pipe sizes, leg spacing, and borehole geometry. Hellstrom [14] proposed a model for VGHEs based on borehole thermal resistance. He derived two-dimensional analytic solutions of the borehole with arbitrary numbers of pipes and assumed a uniform temperature on the borehole wall along the entire depth, which is an oversimplification. Zeng et al. [15] developed a quasi three-dimensional model for VGHEs also based on borehole thermal resistance but using an analytical solution of the fluid temperature profiles along the borehole depth. Cui et al. [7] developed a finite element numerical model for the simulation of the VGHE in alternative operation modes over a short time period for ground-coupled heat pump applications. His model showed that the finite line-source model was not capable of modeling the VGHEs within a few hours. Yang et al. [16] used a two-region model of VGHE; and, proposed an updated two-region VGHE analytical model, which was fitted for system dynamic simulation of ground-coupled heat pumps. His model divides the heat transfer region of VGHE into two areas which are coupled by the temperature of the borehole wall at its boundary. Li and Zheng [9] developed a three dimensional numerical method by using an unstructured grid in the cross section and structured grid at the borehole direction. However, he only solved energy equation for fluid side. In order to account for the effect of changing fluid temperature with depth on the thermal process

\* Corresponding author. Tel.: +98 21 82883361; fax: +98 21 88005040.

E-mail addresses: [gheidari@modares.ac.ir](mailto:gheidari@modares.ac.ir),  
[gheidari@alum.mit.edu](mailto:gheidari@alum.mit.edu) (G. Heidarinejad).

## Nomenclature

$\bar{T}_G$	deep ground temperature (°C)
$A_{GS}$	annual amplitude of the surface ground temperature (°C)
$T$	temperature (°C)
$Re_d$	flow Reynolds number
$d_p$	pipe diameter (m)
$n_f$	number of factorial points
$n_0$	number of center points
$n_a$	number of axial points
$Q$	total heat transfer (W/m)
$\dot{m}$	mass flow rate (kg/s)
$H$	Borehole depth (m)
$C_p$	heat capacity (J/kg K)
$u$	velocity (m/s)
$\bar{K}$	averaged thermal conductivity (W/m K)
$k$	turbulence kinetic energy

## Greek symbols

$\tau$	time (day)
$\tau_0$	time lag (day)
$\bar{\alpha}$	averaged thermal diffusivity (m <sup>2</sup> /s)
$\varepsilon$	turbulence dissipation rate
$\mu$	viscosity (kg/s)
$\rho$	density (kg/m <sup>3</sup> )
$\nu$	kinematic viscosity (m <sup>2</sup> /s)
$\eta$	total heat transfer efficiency
$\theta$	heat exchanger efficiency

## Subscripts

$G$	ground
$S$	soil
$GS$	ground surface
$in$	inlet
$Out$	outlet
$f$	fluid
$p$	pipe
$min$	minimum
$Max$	maximum
$b$	Borehole
$\infty$	far-field

## Superscripts

*	dimensionless sign
---	--------------------

in the bore field, he divided the soil into many layers in the vertical direction. Eventually, his model showed good agreement with experimental data. Nam et al. [17] developed a numerical model to predict heat exchange rates for vertical ground-source heat pump systems. Their proposed method estimated the soil properties based on ground investigations. Their results agreed well with experimental data. Michopoulos and Kyriakis [18] developed a new tool based on analytical equations describing the heat exchanged with the ground formation, which is suitable for energy analysis of vertical ground source heat pump systems. Bandyopadhyay et al. [19] proposed analytical solutions, which were based on the equivalent single core method in U-tube heat exchangers. In their study, both the average fluid temperature and borehole boundary temperature have been obtained using the Gaver–Stehfest numerical inversion algorithm. Sayyaadi et al. [20] performed the multi-objective optimization of a vertical ground-source heat pump using an evolutionary algorithm. Their optimization was based on energy and exergy analysis. Sanaye and Niroomand [21] found an

optimum design process of a ground-source heat pump which includes thermal modeling of the system and selection of optimal design parameters but is based on the sensitivity analysis of investment and electricity costs only. Li et al. [22] defined the soil temperature distribution around a U-tube heat exchanger in a multi-function ground-source heat-pump system. He proposed a new multi-function ground-source heat-pump (MFGSHP) system. His simulation was based on inner heat source theory. Also, several previous studies, Thornton et al. [4], Li et al. [5], Gao et al. [6], Cui et al. [7], Lee and Lam [8] and Li and Zheng [9], have been assuming a constant undisturbed ground temperature profile in their research. This assumption does not model the real condition in which the undisturbed ground temperature varies with depth.

In this study, unlike most of the previous research, a variable undisturbed ground temperature profile is assumed. A full three dimensional CFD model is implemented using this assumption. With aid of the CFD results, a second-order response surface methodology (RSM) model is derived using the Central Composite Design (CCD) approach. The RSM model is obtained for the heat transfer efficiency and the heat exchanger efficiency of a VGHE. Based on the derived model, the most important design parameters are determined and the interactions between them are identified. Also from the model equations, the optimum design combination to achieve higher efficiency can be easily identified.

## 2. Modeling approach

A VGHE interacts thermally not only with the grouts in the borehole but also with the surrounding ground formation. For the convenience of modeling, the volume of ground that is affected by the VGHE, or the ground storage volume, can be considered a three dimensional cylinder with a height greater than the depth of the borehole to ensure that the soil at the bottom boundary is not affected by the VGHE during the time of simulation.

A number of assumptions are needed to develop the model. These assumptions are:

- The grout and the ground formation are assumed homogeneous.
- There is no thermal contact resistance at any interface.
- The heat transfer mechanism in the grout and the ground formation is confined to conduction only and the presence of underground water flow is not considered.

By the foregoing assumptions, a full three-dimensional modeling, previously developed by Heidarinejad et al. [23], is used to determine the VGHE performance. The simulation is performed with the aid of a commercial computational fluid dynamics software package, FLUENT. By taking advantage of the symmetry of the geometry and heat transfer process, only half of the ground storage volume and its associated tubes, fluid, and grout are modeled (as shown in Fig. 2). More details can be found in Heidarinejad et al. [23].

## 3. Undisturbed ground temperature profile

For determination of the thermal interaction of the VGHE with the surrounding ground, precise knowledge of the ground temperature distribution is required. The ground temperature is mainly affected by variations in air temperature and solar radiation. Under influence of these effects, the undisturbed ground temperature fluctuates daily and annually. The annual variation in surface ground temperature can be estimated using a sinusoidal function (Eq. (1)).

$$T(0, \tau) = \bar{T}_G + A_{GS} \cos \left( \frac{2\pi}{365} (\tau - \tau_0) \right) \quad (1)$$

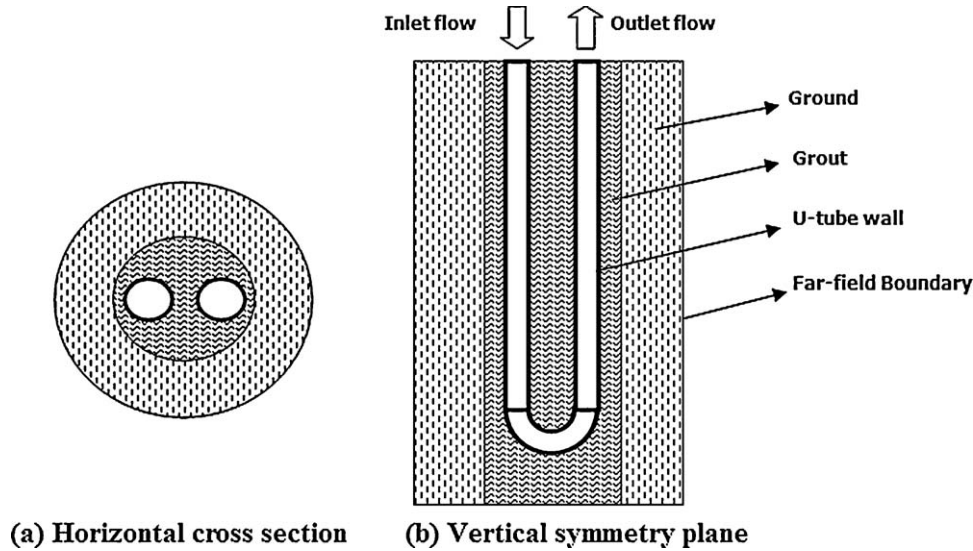


Fig. 1. Schematic diagram of a vertical U-tube ground heat exchanger.

The Kusuda formula [24] (Eq. (2)) which is based on the solution of one-dimensional transient heat conduction in semi-infinite solid with sinusoidal surface temperature, is presented as follow:

$$T(Z, \tau) = \bar{T}_G + A_{GS} \exp \left( -Z \sqrt{\frac{\pi}{365 \alpha_s}} \right) \cos \left( \frac{2\pi}{365} \left( \tau - \tau_0 - \frac{Z}{2} \sqrt{\frac{365}{\pi \alpha_s}} \right) \right) \quad (2)$$

where  $T(Z, \tau)$  is the undisturbed ground temperature at time ( $\tau$ ) and depth ( $Z$ ),  $\bar{T}_G$  is the deep ground temperature which is defined from geological examinations,  $A_{GS}$  is the annual amplitude of the

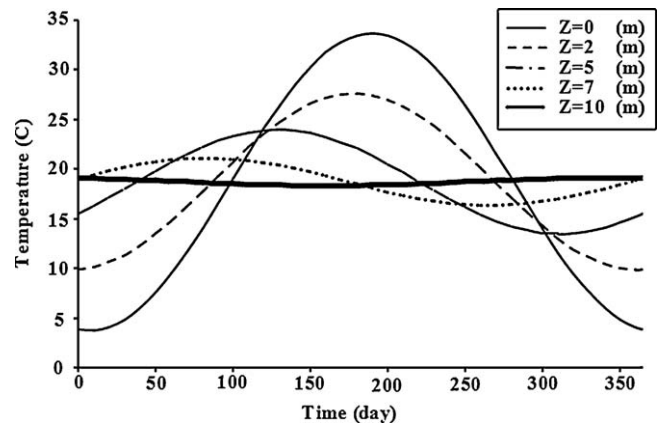


Fig. 3. Ground temperature profile at different depth.

ground surface temperature,  $\tau_0$  is a time lag (days) from an arbitrary starting date, and  $\alpha_s$  is the average thermal diffusivity of soil. When this equation is used for the short period simulation the parameters' unites, such as thermal diffusivity's unit and time's unit, should be converted to the short term format.

As seen in Fig. 3, the undisturbed ground temperature is changing in shallow regions (until 10 m in depth) and after that the ground temperature becomes constant.

In most of previous researches in the field of VGHE modeling, the ground temperature was assumed to be constant in all depth. By this assumption, the ground temperature distribution in the shallow region is inaccurately predicted and consequently, the VGHE performance will be erroneously calculated. So, in order to untangle the mentioned knot, this study assumes the undisturbed ground temperature varies with depth (Eq. (2)).

#### 4. CFD simulation

In order to obtain an accurate prediction of the complex heat transfer process, a full three-dimensional model was performed using the commercial computational fluid dynamics software FLU-ENT. As seen in Fig. 4, because of symmetry in the geometry, the computational grid is generated only for half of the complete domain. The radius of the cylinder has to be chosen carefully to ensure that the soil at the edge is not affected by the VGHE



Fig. 2. Schematic diagram of the computational domain.



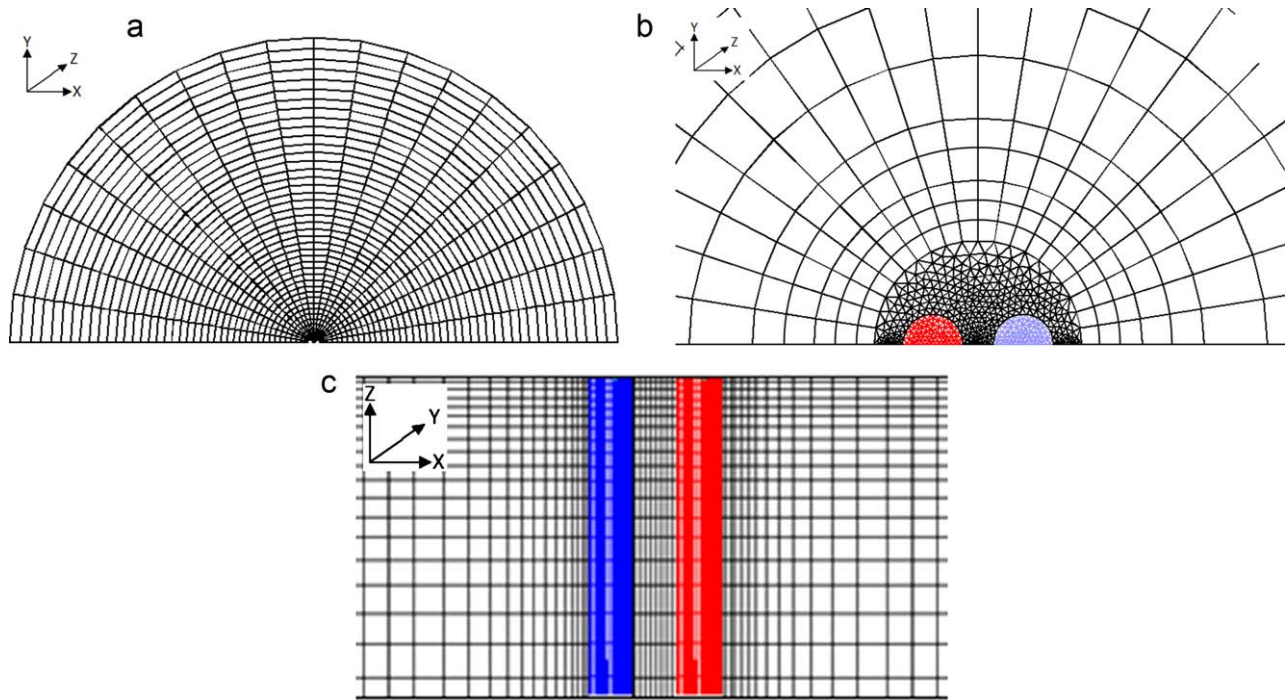


**Fig. 4.** (a) Meshed model of the borehole domain. (b) Magnification of the mesh neighboring to the U-tube. (c) Computational grid of the vertical symmetry plane domain.

during the time of simulation. Hart and Couvillion [25] state that the correct value of  $r_\infty$  is infinity. However, in numerical simulations, the infinity radius is not acceptable and the computational domain should be restricted. They suggested the following equation for defining the far-field radius:

$$r_\infty = 4\sqrt{\alpha_G \tau_{\text{period}}} \quad (3)$$

where,  $r_\infty$  is far-field radius,  $\alpha_G$  is ground diffusivity and  $\tau_{\text{period}}$  is the operation period. In our study, the far-field radius is calculated based on a four-month operation of VGHE. Therefore, the far field radius is defined from Eq. (3). The pressure–velocity coupling in the flow region is determined using the Semi Implicit Method for Pressure Linked Equations (SIMPLE) algorithm. The second order upwind differencing scheme is used to evaluate the advection terms for the Navier–Stokes equations, the energy equation, and the turbulent transport equations. In order to reach the stable temperature variation, along the fluid flow and the return temperature, an unsteady state simulation was performed. For the unsteady simulations, 4 h time periods were used. Stable results are obtained within this period. The unsteady simulations were performed with varied time-steps: 0.01 s, 0.1 s, and 1.0 s in the order specified.

Two objectives of this paper were to quantify the total heat transfer efficiency and heat exchanger efficiency of VGHE. All models have been built using the same approach. Physical properties are provided in Table 1.

## 5. Response surface methodology

Response surface methodology (RSM) is composed of a series of statistical and mathematical methods for analyzing empirical results. When an experiment is performed, the RSM can determine the relationship between output responses (output parameters) and input parameters [26]. RSM was used to analyze the experimental data and to optimize the numerical methods such as CFD. The difference between these two types of usage is in the type of errors that are generated by the responses [27]. In

experimental methods, inaccuracy in results is caused by the measurement errors; whereas, in numerical methods, errors may due to round-off errors or artificial errors. In RSM, the errors are assumed to be random [26]. The RSM consists of correlating the  $N$  variables put into action through a second-order polynomial expression of the following form:

$$\lambda = b_0 + \sum_{i=1}^N (b_i x_i) + \sum_{i=1}^{N-1} \sum_{j=i+1}^N (b_{ij} x_i x_j) + \sum_{i=1}^N (b_{ii} x_i^2) \quad (4)$$

where  $\lambda$  is a response variable, and  $x_i$  the factors or variables which we wish to correlate and the symbols  $b_0$ ,  $b_i$ ,  $b_{ij}$  are constants.

In this study to create an accurate second-order Response Surface Model the Central Composite Design (CCD) method is used. Box and Wilson first described the CCD method in 1951. Today it is one of the most popular second-order models. Each design consists of a standard first order design with  $n_f$  factorial points and  $n_0$  center points, augmented by  $n_a$  axial points (Fig. 5). The factorial points are used to fit linear and interaction terms and the axial points provide additional levels of the factor for the purpose of estimating the quadratic terms. The resulting values, for each of the variables, are used to determine the coefficients of the polynomial equation ( $b_0$ ,

**Table 1**  
Physical material properties.

Property	Value
Soil thermal conductivity (W/m K)	1.83
Soil density ( $\text{kg m}^{-3}$ )	2000
Soil specific heat capacity ( $\text{J kg}^{-1} \text{K}^{-1}$ )	1400
Soil thermal diffusivity ( $\text{m}^2 \text{day}^{-1}$ )	0.05664
Grout thermal conductivity (W/m K)	1.95
Grout density ( $\text{kg m}^{-3}$ )	2500
Grout specific heat capacity ( $\text{J kg}^{-1} \text{K}^{-1}$ )	850
HDPE thermal conductivity (W/m K)	0.42
HDPE density ( $\text{kg m}^{-3}$ )	1100
HDPE specific heat capacity ( $\text{J kg}^{-1} \text{K}^{-1}$ )	1465

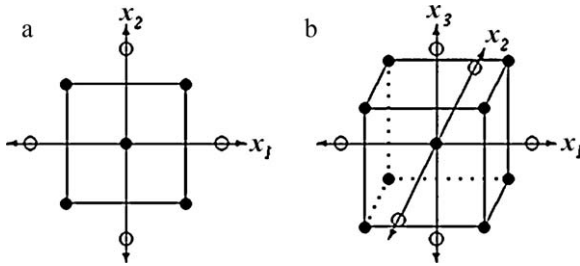


Fig. 5. (a) Two-factor Central Composite Design model. (b) Three-factor Central Composite Design model [27].

$b_i, b_{ij}$ ) and the equation simplified according to the influence of the factors in the final response [27].

## 6. Results and discussions

### 6.1. CFD results

With the aid of the three dimensional numerical simulation, the outlet fluid temperature ( $T_{Out}$ ) is defined and the total heat transfer per unit length ( $Q$ ) is calculated using Eq. (5):

$$Q = \frac{\dot{m}_f C_p (T_{in} - T_{Out}^{CFD})}{H} \quad (5)$$

Several parameters, called design parameters, affect the VGHE outlet fluid temperature ( $T_{Out}^{CFD}$ ). These design parameters are divided in two groups, controllable parameters and uncontrollable parameters. Some controllable parameters, which could affect the VGHE efficiencies, include inlet flow velocity  $u_{in}$ , inlet flow temperature  $T_{in}$ , pipe diameter  $d_p$ , borehole diameter  $d_b$ , borehole depth  $H$ , and the fluid kinematic viscosity  $\nu_f$ . Some uncontrollable design parameters are the ground thermal conductivity ( $\bar{K}_G$ ) and deep ground temperature ( $\bar{T}_G$ ). While the ground thermal conductivity is an uncontrollable parameter, its variation is small for a wide range of ground formations, and thus, ground conductivity is assumed constant in all simulations. By introducing the following dimensionless parameters, the number of design parameters is decreased

$$d_p^* = \frac{d_p}{d_b} \quad H^* = \frac{H}{d_b} \quad T_{in}^* = \frac{T_{in}}{\bar{T}_G} \quad Re_d = \frac{u_{in} d_p}{\nu_f} \quad (6)$$

and, the outlet fluid temperature becomes a function of the design parameters. In other words, the heat exchanger efficiency ( $\theta$ ) is a function of new dimensionless variables:

$$\theta = \frac{T_{in} - T_{Out}^{CFD}}{T_{in} - \bar{T}_G} \quad (7)$$

$$\theta = \Psi(d_p^*, H^*, T_{in}^*, Re_d) \quad (8)$$

In order to understand the complex relationship between the heat exchanger efficiency and design parameters, several simulations were performed using the combination of design parameters specified in Table 2.

Theoretically, the maximum heat transfer occurs when the outlet temperature equals the deep ground temperature, the mass

Table 2  
Range of design parameters used in the RSM.

Design parameter	Min	Mid	Max
$H^*$	120	300	600
$T_{in}^*$	1.75	2	2.5
$Re_d$	3200	6400	9600
$d_p^*$	0.2	0.25	0.3334

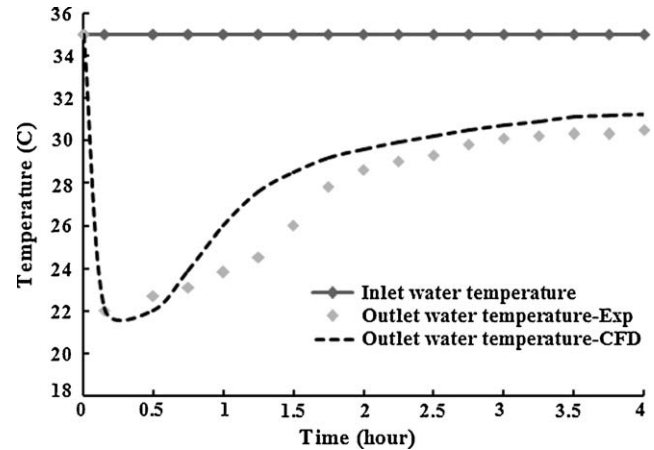


Fig. 6. Comparison of CFD simulated results for outlet fluid temperature with Dobson experiment data [28].

flow rate is at the maximum value, and the borehole depth is at the minimum value. It is clear that this condition never happened in a single VGHEs but this indicator could help to determine an accurate comparison between different VGHEs using the different design parameters. Therefore, the maximum total heat transfer can be expressed as Eq. (9):

$$Q_{Max} = \frac{(\dot{m}_f)_{Max} C_p (T_{in} - \bar{T}_G)}{(H)_{min}} = \left(\frac{\pi}{4}\right) (Re_d)_{Max} \left(\frac{d_p^*}{H^*}\right)_{Max} [\mu C_p (T_{in} - \bar{T}_G)] \quad (9)$$

In order to choose the best combination of design parameter through the presented ranges in Table 2, the dimensionless total heat transfer efficiency is introduced as Eq. (10):

$$\eta = \frac{Q}{Q_{max}} \quad (10)$$

It should be mentioned that the  $\eta$  has not any physical meaning and it is just an intermediate parameter which helps to choosing the best combination of design parameters.

### 6.2. Validation of the numerical results

The CFD results have been constantly verified with experimental data. Thus, the current numerical results were compared to the experimental measurements of Dobson [28]. The experimental setup was installed in Texas, USA and it was consisted of a 67 m deep VGHE with high density polyethylene (HDPE) pipe. The monitored variables included: entering and leaving water temperature of VGHE, water mass flow rate, soil temperature at several depths and radial locations. So, in order to have a tangible sensation of the experiment, its parameters are converted to the proposed non-dimensional format:

$$T_{in}^* = 1.65, \quad d_p^* = 0.2, \quad H^* = 600, \quad Re_d = 8650 \quad (11)$$

In this stage, the short-term behavior of the fluid outlet temperature was compared experimentally and numerically every 2 min for the first 0.5 h.

As seen in Fig. 6, the maximum difference between the CFD results and experimental data is about 3.5%, so it is reasonable to say that the outlet fluid temperature shows reasonable agreement with experimental results.

Both the simulation and the experiment have the same conditions. Only the soil thermal diffusivity, which is used in the simulation, has a mean value inferred from the thermal response test [28].

**Table 3**  
CFD simulation results and predicted RSM model values for two response variables ( $\theta$  and  $\eta$ ).

Test number	$H^*$	$T_{in}^*$	$Re_d$	$d_p^*$	$\theta$		$\eta$	
					CFD	2nd RSM	CFD	2nd RSM
1	120	2.5	3200	0.3334	0.2033	0.21548	0.0697	0.0705
5	300	1.75	6400	0.2	0.1466	0.1425	0.0284	0.0302
9	600	2	9600	0.2	0.1233	0.1312	0.0157	0.0165
14	600	1.75	6400	0.2	0.2500	0.2369	0.0199	0.0175
18	300	2	9600	0.3334	0.0766	0.0882	0.0306	0.0325
23	600	2.5	6400	0.25	0.1966	0.1960	0.0176	0.0165
27	300	2.5	9600	0.2	0.1100	0.1025	0.0263	0.0270
30	600	2.5	6400	0.2	0.3233	0.3388	0.0248	0.0237

By using Design-Expert 7.1 software packages, the simulation conditions of 30 tests were generated which some model tests are shown in Table 3 for instance.

Based on these testing conditions, the heat transfer efficiency and the heat exchanger efficiency (response variables) are computed from the CFD that was described earlier in Section 6.2. The CFD-predicted  $\eta$  and  $\theta$  values and the predictions from the RSM are plotted in Fig. 7 for different test numbers.

### 6.3. Development of second-order model

After doing the 30 numerical runs using CFD, the simulated results for the total heat transfer efficiency and the heat exchanger efficiency are used to find the model parameters used in the second-order RSM model (see Eqs. (12) and (13)). In order to calculate the parameters, the CCD approach is used. The second-order model for

predicting  $\eta$  and  $\theta$  can be expressed as:

$$\begin{aligned} \eta = & -0.10699 \\ & -3.231 \times 10^{-4}(H^*) + 0.054015(T_{in}^*) \\ & + 1.25045 \times 10^{-5}(Re_d) + 0.74401(d_p^*) \\ & + 2.34584 \times 10^{-5}(H^*)(T_{in}^*) + 3.12746 \times 10^{-9}(H^*)(Re_d) \\ & - 2.46997 \times 10^{-4}(H^*)(d_p^*) - 2.13490 \times 10^{-7}(T_{in}^*)(Re_d) \\ & - 0.16627(T_{in}^*)(d_p^*) - 5.28118 \times 10^{-6}(Re_d)(d_p^*) \\ & + 2.87387 \times 10^{-7}(H^*)^2 - 4.94207 \times 10^{-3}(T_{in}^*)^2 \\ & - 8.81669 \times 10^{-10}(Re_d)^2 - 0.25651 \times 10^{-10}(d_p^*)^2 \end{aligned} \quad (12)$$

$$\begin{aligned} \theta = & -0.31014 \\ & -2.80172 \times 10^{-4}(H^*) + 0.30673(T_{in}^*) \\ & - 4.90586 \times 10^{-6}(Re_d) + 1.39860(d_p^*) \\ & + 3.51581 \times 10^{-5}(H^*)(T_{in}^*) + 8.27061 \times 10^{-9}(H^*)(Re_d) \\ & + 7.37015 \times 10^{-5}(H^*)(d_p^*) - 2.37669 \times 10^{-7}(T_{in}^*)(Re_d) \\ & - 0.22829(T_{in}^*)(d_p^*) - 3.96615 \times 10^{-5}(Re_d)(d_p^*) \\ & + 3.88545 \times 10^{-7}(H^*)^2 - 0.058935(T_{in}^*)^2 \\ & - 4.05168 \times 10^{-10}(Re_d)^2 - 1.34967(d_p^*)^2 \end{aligned} \quad (13)$$

From examining these expressions and the values of the coefficients, one can easily deduce that the response variables ( $\eta$  and  $\theta$ ) are significantly affected by the dimensionless inlet fluid temperature ( $T_{in}^*$ ) and dimensionless pipe diameter ( $d_p^*$ ) but are weakly affected by the dimensionless depth ( $H^*$ ). In addition, it is interesting to note that interaction of dimensionless inlet fluid temperature ( $T_{in}^*$ ) with the dimensionless pipe diameter ( $d_p^*$ ) is major while the interactions with other design parameters are at a minor level, as deduced from second-order RSM model.

As seen from Fig. 7, the predicted response values obtained from the second-order RSM model agree well with the CFD values.

### 6.4. Optimization

By inspecting the numerical results of the total heat transfer efficiency ( $\eta$ ) and the heat exchanger efficiency ( $\theta$ ), it is found that these two responses are varied when the design parameters change. For example, as the depth of borehole is increased, the heat exchanger efficiency is increased; but the total heat transfer efficiency is decreased. Thus, their behaviors are not distinctly predictable when the design parameter varies. Thus, there exists a position where both responses are optimized. Optimization was performed, using Design-Expert 7.1 software, with the condition that both responses should be at the maximum value at the same time, and other design parameter must be situated within the range of the design parameters.

The second order RSM models were optimized at  $\eta = 0.046289$  and  $\theta = 0.248792$ , subject to the following combination of design variables:

$$H^* = 278.83, \quad T_{in}^* = 1.91, \quad d_p^* = 0.3334, \quad \text{and} \quad Re_d = 3200 \quad (14)$$

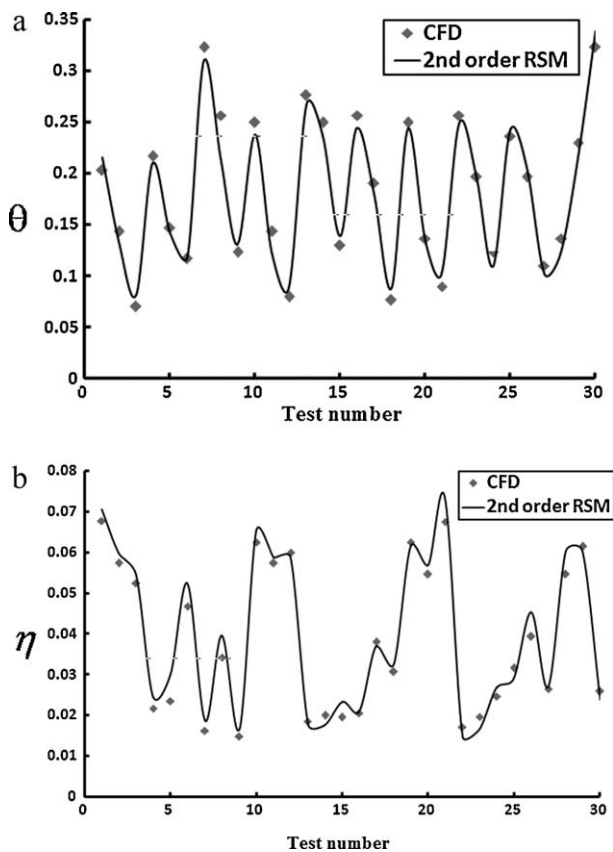


**Fig. 7.** Comparison of 2nd order RSM against CFD predictions. (a) Heat exchanger efficiency. (b) Heat transfer efficiency.

In order to verify the optimized  $\eta$  and  $\theta$  values predicted from RSM, the CFD simulation was performed again using the combination of design variables shown in Eq. (14); the computed  $\eta$  and  $\theta$  are 0.043658 and 0.26984 (Error $_{\eta}$  = 5.6% and Error $_{\theta}$  = 8.4%). The computed CFD values favorably agree with predicted value from RSM optimization.

## 7. Conclusion

In this paper, unlike most previous simulations, a full three dimensional computational fluid dynamics simulation with approximately 3.5% error was performed. The highly accurate RSM model was used to show how design parameters could simultaneously affect the response variables. The effect of four dimensionless design parameters  $H^*$ ,  $T_{in}^*$ ,  $d_p^*$ ,  $Re_d$  on two dimensionless response variables  $\eta$  and  $\theta$  was examined. In order to understand the complex relationship between design parameters and response variables, the second order Response Surface Model with Central Composite Design approach has been used. Results conclude that the response variables are strongly affected by the dimensionless inlet fluid temperature ( $T_{in}^*$ ) and the dimensionless pipe diameter ( $d_p^*$ ) but are weakly affected by dimensionless depth ( $H^*$ ). The interaction of the dimensionless inlet fluid temperature ( $T_{in}^*$ ) with the dimensionless pipe diameter ( $d_p^*$ ) is at a major level while the interactions with other design parameters are at a minor level, as determined from the values of the coefficients. The optimum combination needed to reach the optimum response variable is determined.

## References

- [1] V.C. Mei, C.J. Emerson, New approach for analysis of ground-coil design for applied heat pump system, *ASHRAE Transactions* 91 (1985) 1216–1224.
- [2] N.K. Muraya, D.L. O'Neal, W.M. Heffington, Thermal interference of adjacent legs in vertical U-tube heat exchanger for a ground-coupled heat pump, *ASHRAE Transactions* 102 (1996) 12–21.
- [3] S.P. Rottmayer, W.A. Beckman, J.W. Mitchell, Simulation of a single vertical U-tube ground heat exchanger in an infinite medium, *ASHRAE Transactions* 103 (1997) 651–659.
- [4] J.W. Thornton, T.P. McDowell, J.A. Shonder, P.J. Hughes, D. Pahud, G. Hellstrom, Residential vertical geothermal heat pump system models: calibration to data, *ASHRAE Transactions* 103 (1997) 660–674.
- [5] X.G. Li, Z.H. Chen, J. Zhao, Simulation and experiment on the thermal performance of U-vertical ground coupled heat exchanger, *Applied Thermal Engineering* 26 (2006) 1564–1571.
- [6] J. Gao, X. Zhang, J. Liu, K.S. Li, J. Yang, Thermal performance and ground temperature of vertical pile-foundation heat exchangers: a case study, *Applied Thermal Engineering* 28 (2008) 2295–2304.
- [7] P. Cui, H. Yang, Z. Fang, Numerical analysis and experimental validation of heat transfer in ground heat exchangers in alternative operation modes, *Energy and Buildings* 40 (2008) 1060–1066.
- [8] C.K. Lee, H.N. Lam, Computer simulation of borehole ground heat exchangers for geothermal heat pump systems, *Renewable Energy* 33 (2008) 1286–1296.
- [9] Z. Li, M. Zheng, Development of a numerical model for the simulation of vertical U-tube ground heat exchangers, *Applied Thermal Engineering* 29 (2009) 920–924.
- [10] S.P. Kavanaugh, Simulation and experimental verification of vertical ground coupled heat pump systems, Ph.D. Dissertation, Oklahoma State University, USA, 1984.
- [11] P. Eskilson, J. Claesson, Simulation model for thermally interacting heat extraction boreholes, *Numerical Heat Transfer* 13 (1988) 149–165.
- [12] C. Yavuzturk, J.D. Spitler, S.J. Rees, A transient two-dimensional finite volume model for the simulation of vertical U-tube ground heat exchangers, *ASHRAE Transactions* 105 (2) (1999) 465–474.
- [13] C. Yavuzturk, J.D. Spitler, S.J. Rees, Short time step response factor model for vertical ground loop heat exchangers, *ASHRAE Transactions* 105 (1999) 475–485.
- [14] G. Hellstrom, Ground heat storage: thermal analysis of duct storage systems, Doctoral Thesis, Department of Mathematical Physics, University of Lund, Lund, Sweden, 1991.
- [15] H. Zeng, N. Diao, Z. Fang, Heat transfer analysis of boreholes in vertical ground heat exchangers, *International Journal of Heat and Mass Transfer* 46 (2003) 4467–4481.
- [16] W. Yang, M. Shi, G. Liu, Z. Chen, A two-region simulation model of vertical U-tube ground heat exchanger and its experimental verification, *Applied Energy* 86 (2009) 2005–2012.
- [17] Y. Nam, R. Ooka, S. Hwang, Development of a numerical model to predict heat exchange rates for a ground-source heat pump system, *Energy and Buildings* 40 (2008) 2133–2140.
- [18] A. Michopoulos, N. Kyriakis, A new energy analysis tool for ground source heat pump systems, *Energy and Buildings* 4 (2009) 937–941.
- [19] G. Bandyopadhyay, W. Gosnold, M. Mann, Analytical and semi-analytical solutions for short-time transient response of ground heat exchangers, *Energy and Buildings* 40 (2008) 1816–1824.
- [20] H. Sayyaadi, E. Hadaddi Amlashi, M. Amidpour, Multi-objective optimization of a vertical ground source heat pump using evolutionary algorithm, *Energy Conversion and Management* 50 (2009) 2035–2046.
- [21] S. Sanaye, B. Niroomand, Thermal-economic modeling and optimization of vertical ground-coupled heat pump, *Energy Conversion and Management* 50 (2009) 1136–1147.
- [22] S. Li, W. Yang, X. Zhang, Soil temperature distribution around a U-tube heat exchanger in a multi-function ground source heat pump system, *Applied Thermal Engineering* 29 (2009) 3679–3686.
- [23] G. Heidarinejad, V. Khalajzadeh, S. Delfani, Performance analysis of a ground assisted direct evaporative cooling air conditioner, *Building and Environment* 45 (10) (2010) 2327–2335.
- [24] T. Kusuda, P.R. Archenbach, Earth temperature and thermal diffusivity at selected stations in the United States, *ASHRAE Transactions* 71 (1) (1965) 61–74.
- [25] D.P. Hart, R. Couvillion, Earth-coupled Heat Transfer, National Water Well Association, Dublin, OH, 1986, pp. 11–16.
- [26] A. Dean, D. Voss, Design and Analysis of Experiments, Springer, 1999, p. 562.
- [27] A.I. Khuri, Response Surface Methodology and Related Topics, Word Scientific Publishing Co, 2006, p. 257.
- [28] M.K. Dobson, an experimental and analytical study of the transient behavior of vertical U-tube ground-coupled heat pumps in the cooling mode, M.S. Thesis, Texas A&M University, 1999.